pH Dependencies of the *Tetrahymena* Ribozyme Reveal an Unconventional Origin of an Apparent pK_a[†]

Deborah S. Knitt and Daniel Herschlag*

Department of Biochemistry, B400 Beckman Center, Stanford University, Stanford, California 94305-5307

Received September 5, 1995; Revised Manuscript Received December 1, 1995[⊗]

ABSTRACT: The L-21 *Sca*I ribozyme derived from the *Tetrahymena thermophila* pre-rRNA group I intron catalyzes a site-specific endonucleolytic cleavage of RNA, DNA, and chimeric RNA/DNA oligonucleotides: $CCCUCUA_5 + G \rightarrow CCCUCU + GA_5$. The pH−rate dependence was determined for the reaction of the E·G complex with the oligonucleotide substrate d(CCCUC)r(U)d(A_5) [$(k_{cat}/K_m)^S$ conditions]. Although it was shown that the pH dependence is not affected by specific buffers, there is inhibition by specific monovalent cations. The intrinsic pH−rate dependence is log−linear with slope 1 below pH 7, displays an apparent pK_a of 7.6, remains nearly level until pH 8.5, and then begins to fall. Two models to explain the apparent pK_a were ruled out: (1) the pK_a represents loss of a proton from the nucleophilic 3′ OH of G, and (2) the pK_a arises from a change in rate-limiting step from a pH-dependent to a pH-independent step. In addition, these models, or others involving a single titration, cannot account for the decrease in activity at high pH. A third, unconventional, model is consistent with all of the data. It involves inactivation of the ribozyme by any of several independent titrations of groups with pK_a values considerably higher than the apparent pK_a of 7.6. The data are consistent with loss of catalytic function upon release of a proton from any one of 19 independent sites with pK_a = 9.4 (the unperturbed pK_a of N1 of G and N3 of U in solution). Independent experiments investigating the effect of pH on different reaction steps supported this model and suggested the identity of some of the required protons. This mechanism of inactivation is expected to generally affect the behavior of RNAs at pH values removed from the pK_a of the titrating bases.

In 1982, Cech and co-workers discovered that a group I RNA intron from *Tetrahymena thermophila* pre-rRNA was capable of catalyzing its own excision from the 5′ and 3′ exons (Kruger et al., 1982). This discovery revealed that macromolecular catalysis is not exclusive to proteins and that RNA is capable of stabilizing a transition state. Studying RNA catalysis, however, presents different problems than studying protein catalysis. RNA contains four very similar building blocks, each with titratable groups, whereas proteins contain 20 varied building blocks, only some of which contain titratable groups. The backbones of each molecule also greatly differ, with proteins containing polar amide linkages and RNA containing negatively charged phosphodiester linkages. These differences suggest that pH, specific ions, and ionic strength may have larger effects on RNA catalysis than on protein catalysis.

This paper addresses these issues with a ribozyme derived from the *Tetrahymena* intron and provides general insight into how pH can affect RNA catalysis and function. The results suggest that titration of multiple independent protons that are required for activity collaborate to give an apparent pK_a considerably lower than that of the individual functional groups. This mechanism of inactivation will likely be observed for other RNA catalysts and functional RNAs.

MATERIALS AND METHODS

Materials. L-21 *Sca*I ribozyme was prepared by *in vitro* transcription and purified as described previously (Zaug et al., 1988). The analogous ribozyme beginning with a 5′-OH instead of the 5′-triphosphate was kindly provided by Scott Strobel. Oligonucleotides were made by solid phase synthesis and were supplied by the Protein and Nucleic Acid Facility at Stanford University or by Clontech (Palo Alto, CA), or were used and characterized in previous studies. Oligonucleotides were purified by nondenaturing polyacrylamide gel electrophoresis and characterized subsequent to 5′-end-labeling with [γ-^{32}P]ATP using T4 polynucleotide kinase as described previously (Zaug et al., 1988; Herschlag et al., 1993a). Ribozyme was 5′-end-labeled and purified by denaturing polyacrylamide gel electrophoresis subsequent to removal of the 5′-triphosphate with calf intestinal phosphatase (Zaug et al., 1988; Latham & Cech, 1989).

General Kinetic Methods. All reactions were single turnover, with ribozyme (E)[1] in excess of 5′-end-labeled substrate (S*, ∼0.1 nM) and unless otherwise stated were

[†] This work was supported by NIH Grant GM49243 to D.H. D.H. is a Lucille P. Markey Scholar in Biomedical Sciences and a Searle Scholar (Chicago Community Trust). D.S.K. was supported by an NSF Predoctoral Fellowship.

* To whom correspondence should be addressed. Phone: (415) 723-9442. FAX: (415) 723-6783. E-mail: herschla@cmgm.stanford.edu.

[⊗] Abstract published in *Advance ACS Abstracts,* January 15, 1996.

[1] Abbreviations: S is used to generically refer to the oligonucleotide substrate, CCCUCUAAAAA, without specification of the sugar identity. S* represents 5′ end-labeled oligonucleotide substrate. The individual substrates investigated are defined in Chart 1. E is the L-21 *Sca*I ribozyme; P1 is the helix formed between the internal guide sequence (IGS) of the ribozyme and the oligonucleotide substrate or product (see Figure 7); IGS′ is the all-ribose oligonucleotide GGAGGGA, which has the sequence of the ribozyme's IGS; MES, 2-(*N*-morpholino)-ethanesulfonic acid; EPPS, *N*-(2-hydroxyethyl)piperazine-*N*′-3-propanesulfonic acid; MOPS, 3-(*N*-morpholino)propanesulfonic acid; HEPES, *N*-(2-hydroxyethyl)piperazine-*N*′-2-ethanesulfonic acid; CHES, (cyclohexylamino)ethanesulfonic acid.

0006-2960/96/0435-1560$12.00/0

carried out in 50 mM buffer, and 10 mM $MgCl_2$ at 50 °C as described previously (Herschlag & Cech, 1990; Herschlag et al., 1993a). Briefly, reactions were initiated by addition of S following a 15 min/50 °C preincubation of E in $MgCl_2$ and buffer. Six aliquots of 1−2 μL were removed from 20 μL reactions at specified times, and further reaction was quenched by the addition of ∼2 volumes of 20 mM EDTA in 90% formamide with 0.005% xylene cyanole, 0.01% bromophenol blue, and 1 mM Tris, pH 7.5. Substrates and products were separated by electrophoresis on 20% polyacrylamide/7 M urea gels, and their ratios at each time point were quantitated with a Molecular Dynamics PhosphorImager. Reactions were typically followed for ∼3$t_{1/2}$, except for the slowest reactions, which were followed for times such that there was no indication of inactivation of E from curvature in reaction progress curves or from loss of activity in control reactions in which E was incubated under reaction conditions for varying times prior to initiation of a reaction that is first order in E concentration ["$(k_{cat}/K_m)^S$ conditions"]. The disappearance of S was first order, and endpoints of ∼95% were typically obtained in nonlinear least-squares fits (KaleidaGraph, Synergy Software, Reading, PA). If only initial rates could be measured, an endpoint of 95% was assumed. There was one exception to the endpoint of 95%. The phosphorothioates studied had endpoints of ∼50%. These substrates have sulfur replacing a nonbridging phosphoryl oxygen atom at the cleavage site. They were used as a mixture of the R_p and S_p isomers, but only the R_p substrate reacts on the time scale of these experiments (Rajagopal et al., 1989; Herschlag et al., 1991; J. A. Piccirilli and T. R. Cech, personal communication). Details of specific kinetic experiments are described in the following sections. The pH dependencies were fitted using SigmaPlot (Jandel Scientific).

The buffers used in these experiments (and their pH values at 50 °C) were as follows: sodium acetate (5.6); NaMES (5.2−6.7); NaHEPES (6.5−7.8); NaMOPS (6.8−7.8); NaEPPS (6.9−8.8); NaCHES (8.0−9.5). Typically, the pH was measured at 25 °C and corrected to 50 °C using the following factors: sodium acetate, no change; NaMES, −0.2; NaHEPES, -0.3; NaMOPS, −0.3; NaEPPS, −0.3; NaCHES, −0.6. These correction factors were obtained by measuring the pH at 25 and 50 °C for each buffer at select pH values and agree reasonably well with those previously reported (Good et al., 1966; Gueffroy, 1978).

Kinetic Constants. The following nomenclature is used for kinetic constants. $(k_{cat}/K_m)^S$ represents the second-order rate constant for reaction of E·G + S → products, and $(k_{cat}/K_m)^G$ represents the second-order rate constant for reaction of E·S + G → products. Values of $(k_{cat}/K_m)^S$ were obtained with 2 mM G, which is nearly saturating at pH ≤ 8.5 ($K_m^G \approx 1$ mM; these reported values are 30%−40% below the values obtained by extrapolation to saturating G). Binding of G is weaker at pH > 8.5 (*vide infra*), and the limited solubility of G prevented determination of the higher K_m^G values. Thus, the rate constants in pH−rate profiles that include reactions at pH > 8.5 are referred to as $(k_{cat}/K_m)^{S,app}$ to indicate that 2 mM G is not saturating over the entire pH range. These reactions are depicted with G in parentheses, E·(G) + S → products, again to signify that G is not saturating over the entire pH range. This problem with G saturation does not affect the observed pK_a of 7.6, nor does it affect the tests of models I and II presented in the Results, as only measurements at pH ≤ 8.5 are invoked. For model III, it was necessary to include the data obtained at pH > 8.5. The absence of saturation over the entire pH range influences the quantitative interpretation but not the qualitative conclusion. In addition, the pH dependence for the third-order reaction of E + S + G had the same overall shape as that for $(k_{cat}/K_m)^{S,app}$ (data not shown).

Chart 1

abbreviation	oligonucleotide substrate (-5 -3 -1 +2 +4)
-1r,dS	dC dC dC dU dC rU dA dA dA dA dA
dS	dC dC dC dU dC dU dA dA dA dA dA
-1d,rS	rC rC rC rU rC dU rA rA rA rA rA
-1r,-$1_{(P\text{-}S)}$,dS	dC dC dC dU dC $rU_{(P\text{-}S)}$ dA dA dA dA dA
-$1_{(P\text{-}S)}$,dS	dC dC dC dU dC $dU_{(P\text{-}S)}$ dA dA dA dA dA

The term K_m is used to define the concentration of ribozyme, G, or S that provides half of the maximal rate, even though the reactions are single turnover and therefore not under steady state conditions. This nomenclature is used to emphasize that this value does not *a priori* equal an equilibrium dissociation constant. For each of the saturation curves presented herein, there is strong independent evidence suggesting that K_m^G equals the true equilibrium dissociation constant, K_d^G, as described previously (McConnell et al., 1993). The association constant K_a^G (= $1/K_d^G$) is used in the text for clarity.

Minimization of Enzyme Degradation by the pH Jump Method. The pH jump method consists of an incubation at 50 °C, 12.5 mM $MgCl_2$, and 25 mM NaMES at pH ∼7. Aliquots of these reaction mixtures, 4 μL, were incubated for 15 min at 50 °C and then added to 14 μL of a solution, also at 50 °C, containing the buffer at the pH of the reaction along with varying concentrations of $MgCl_2$ and G. Fifteen seconds after the pH was raised, the radioactive substrate was added in a 2 μL aliquot to generate a final volume of 20 μL. The final concentration of NaMES buffer, initially pH ∼7, was 5 mM, while the final concentration of the high pH sodium buffers was 50 mM. NaMES, pH 7, was chosen for the incubation buffer as it has little buffer capacity at higher pH values and thus did not significantly affect the pH following the jump. This protocol gave the same rate constants as were obtained in reactions carried out without the pH jump for reactions carried out at intermediate pH.

Further Controls for Ribozyme Degradation at High pH. In addition to utilization of the pH jump method described above to minimize degradation at high pH values, other controls were carried out to ensure the validity of the rate constants measured at high pH values. These controls included (1) ensuring that good first-order kinetics were followed, (2) preincubating the ribozyme at the reaction pH for differing lengths of time to ensure that there is no change in the observed rate constants over the time period of the reaction from time-dependent degradation, and (3) 5′-end-labeling the ribozyme to measure the amount of degradation at the higher pH values; only time points corresponding to less than ∼20% ribozyme degradation were used in the determination of kinetic constants.

pH Dependence for Reaction of −1r,dS. The pH dependence for reaction of −1r,dS (Chart 1) was determined under

$(k_{cat}/K_m)^{S,app}$ conditions, E·(G) + S → products, with the measurements carried out at 50 °C, 50 mM sodium buffer, 100−300 nM E, 2 mM G, ∼0.1 nM −1r,dS, and 10 mM $MgCl_2$ with or without added salts. Several control experiments with varying [E] at several pH values indicated that E was subsaturating [Herschlag et al. (1993a) and data not shown].

pH Dependence for Reaction of −1d,rS. $(k_{cat}/K_m)^G$ was determined for reaction of −1d,rS at 50 °C, 50 mM sodium buffer, 200 nM E, ∼0.1 nM −1d,rS, and 10 mM $MgCl_2$. Guanosine concentrations ranged from 0 to 12 μM, with at least five concentrations used for each $(k_{cat}/K_m)^G$ determination. The G concentrations were chosen to remain at least 5-fold below the dissociation constant of G from the E·S·G complex of ∼100 μM (McConnell et al., 1993). It has previously been shown that the concentration of E is saturating with respect to S over this pH range (Herschlag & Khosla, 1994).

K_a^G Measurements vs pH for Reaction of −1r,dS. Rate constants for reaction of −1r,dS were determined at 50 °C, 50 mM sodium buffer, pH 5.2−8.5, 100 nM E, ∼0.1 nM −1r,dS, and 10 mM $MgCl_2$ with concentrations of G ranging from 0 to 4.6 mM. Under these conditions, the concentration dependence of the rate reflects the actual association constant, K_a^G, as described previously (McConnell et al., 1993). Multiple independent experiments were carried out because determination of K_a^G was limited by the low solubility of G, which prevented use of G concentrations 10-fold above the dissociation constant. G binding at pH values > 8.5 could not be accurately determined due to weaker binding coupled with a higher amount of scatter in the primary data for reactions at high pH.

Determination of the Thio-Effect for Reaction of −1r,dS and dS vs pH. $(k_{cat}/K_m)^S$ was determined at 50 °C, 50 mM sodium buffer, pH 5.6−8.2, 50−300 nM E, 2 mM G, ∼0.1 nM S, and 10 mM $MgCl_2$ for substrates containing either an oxygen or a sulfur at the *pro*-R_p position of the phosphate at the cleavage site [S = −1r,dS; −1r,−1(P−S),dS; dS; or −1(P−S),dS, Chart 1]. The ratio of $(k_{cat}/K_m)^S$ for the phosphate oxygen relative to $(k_{cat}/K_m)^S$ for the phosphorothioate substrate is termed the thio-effect.

Though variations of up to ∼2-fold in individual rate constants have been observed in independent experiments (Herschlag & Cech, 1990), the variation in side-by-side experiments is considerably less. Multiple determinations in each experiment allowed the observed small thio-effects to be distinguished from a thio-effect of 1.0 (see Figure 4 below).

Measurement of Duplex Stabilities by Substrate Inhibition. Duplex stabilities were determined using a method termed substrate inhibition (G. J. Narlikar, M. Khosla, N. Usman, and D. Herschlag, manuscript in preparation). This method involves measuring $(k_{cat}/K_m)^{S,app}$ while adding increasing amounts of the inhibitor, IGS′ (GGAGGGA).[1] The inhibitor competes with the IGS strand on the ribozyme for binding to S and thereby slows reaction of S. Because these reactions were carried out under conditions in which free E, free S, and free IGS′ were in equilibrium, K_I is equal to K_d^S, the duplex stability of the model duplex between IGS and S [see Knitt et al. (1994) and G. J. Narlikar, M. Khosla, N. Usman, and D. Hershlag, manuscript in preparation, for controls).

$(k_{cat}/K_m)^{S,app}$ values for reaction of −1r,dS were determined with 0−300 μM IGS′ at 50 °C, 50 mM sodium buffer, 100 nM E, 2 mM G, and ∼0.1 nM −1r,dS at pH values ranging from 6.6 to 8.9 using the pH jump method to standardize conditions and prevent E degradation. After preincubation of 4 μL of E and G in buffer and $MgCl_2$ at 50 °C for 15 min, 12 μL of a jump was added to increase the pH. Fifteen seconds later, 2 μL of a 10× concentration of IGS′ was added, followed after another 15 s by a 2 μL addition of radioactive substrate to give a final reaction volume of 20 μL. Inhibition curves were obtained with at least six IGS′ concentrations. Concentrations of IGS′ were used that spanned the observed K_d^S value by ∼5−10-fold on either side.

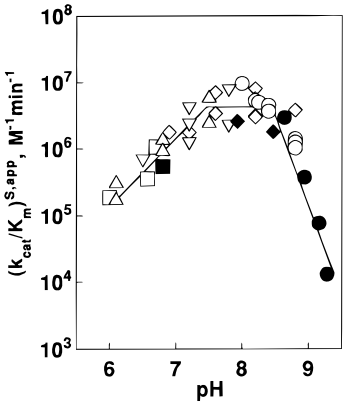

FIGURE 1: pH dependence for cleavage of −1r,dS. The rate constant $(k_{cat}/K_m)^{S,app}$ for the reaction E·(G) + S* → products was determined with the following buffers: MES, □, ■; MOPS, ▽; HEPES, △; EPPS, ◇, ◆; and CHES, ○, ● (50 mM sodium buffer, 2 mM G, 100 nM E, 10 mM $MgCl_2$, 50 °C). The closed symbols represent rate constants obtained via the pH jump method (see Materials and Methods). The second-order rate constant $(k_{cat}/K_m)^{S,app}$ is referred to as "apparent" because G is not saturating at pH > 8.5 (see Materials and Methods). The data represent a compilation from several independent experiments.

RESULTS

pH Dependence of $(k_{cat}/K_m)^{S,app}$ for Reaction of −1r,dS. The −1r,dS substrate was chosen to probe the pH dependence of the ribozyme reaction rather than the standard all-ribose substrate, rS, because previous work revealed an apparent pK_a for rS arising from a change in rate-limiting step (Herschlag & Khosla, 1994). The results described below demonstrate that this complication is avoided with the chimeric substrate. In addition, the role of the individual 2′-OH groups is well established, allowing results obtained with chimeric substrates to be related to the behavior of the all-ribose substrate (Bevilacqua & Turner, 1991; Pyle & Cech, 1991; Herschlag et al., 1993a,b; G. J. Narlikar and D. Herschlag, unpublished results).

$(k_{cat}/K_m)^{S,app}$ vs pH for −1r,dS is shown in Figure 1, representing the reaction E·(G) + S → products. This pH dependence revealed a region with a slope of 1, a leveling off around pH 8, and a drop in reactivity above pH 8.5. However, before this dependence could be interpreted as "intrinsic" to the ribozyme, it had to be determined if the pH dependence arose solely from the changing $[H^+]$, as effects from ionic strength, specific buffers, or specific salts can complicate an observed pH dependence. Such effects might be especially problematic when dealing with a highly charged RNA molecule. As described in the next section, there are no specific buffer effects, whereas specific salts do have differential inhibitory effects. Nevertheless, the pH

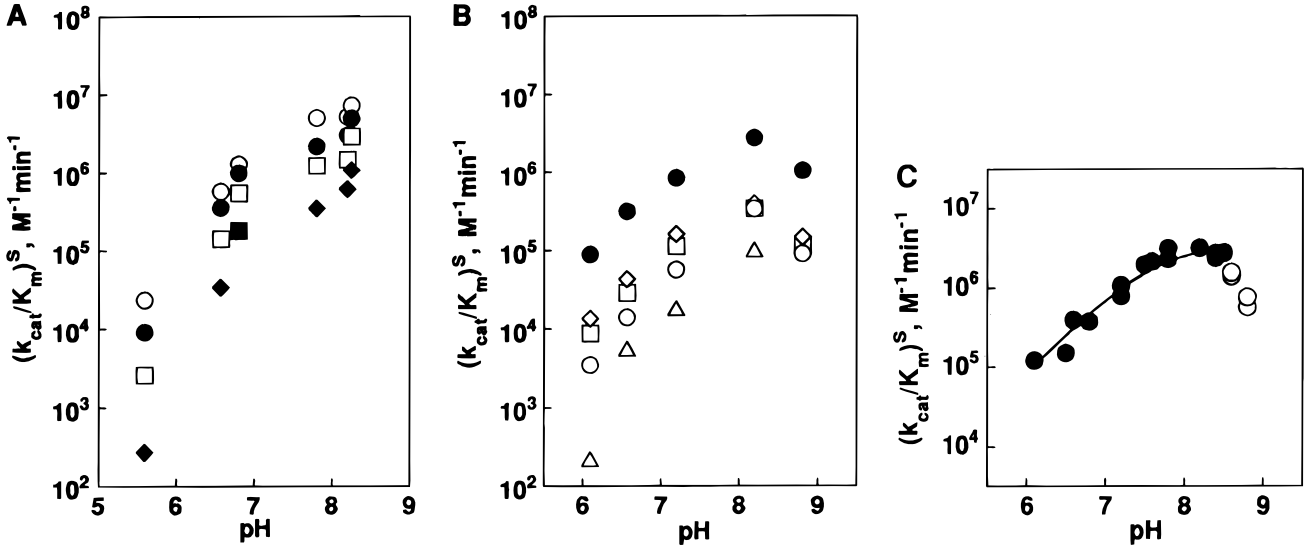

FIGURE 2: Effects of buffer and salt on the observed pH dependence [$(k_{cat}/K_m)^S$, 2 mM G, 100 nM E, 10 mM $MgCl_2$, 50 °C]. (A) Effect of varying concentration of buffers on $(k_{cat}/K_m)^S$. The buffer concentrations used were 25 mM, ○; 50 mM, ●; 100 mM, □; 150 mM, ■; and 200 mM, ◆. The following buffers were used: sodium acetate, pH 5.6; NaMES, pH 6.6; NaMOPS, pH 6.8; NaHEPES, pH 7.8; NaEPPS, pH 8.2; and NaCHES, pH 8.3. (B) Effect of specific salts on $(k_{cat}/K_m)^S$. Reactions were carried out in 50 mM buffer in the absence (●) or presence of 200 mM added salt: RbCl, ◇; KCl, □; NaCl, ○; or LiCl, △. The following buffers were used: NaMES, pH 6.1; NaMES, pH 6.6; NaHEPES, pH 7.2; NaEPPS, pH 8.2; and NaCHES, pH 8.8. (C) Determination of the apparent pK_a under conditions of constant Na^+. Reactions were carried out in 50 mM buffer with NaCl added to give 50 mM total Na^+. The following buffers were used: NaMES, pH 6.1, 6.6; NaMOPS, pH 6.8, 7.8; 7.5, 7.8 NaHEPES, pH 6.5, 7.2; NaEPPS, pH 7.2, 7.6, 8.2, 8.5; and NaCHES, pH 8.4, 8.6, 8.8. The closed symbols represent the data used in a nonlinear least-squares fit to eq 1. The fit gives $(k_{cat}/K_m)^{S'} = 3.5 \times 10^6$ M^{-1} min^{-1} and $K_a = 2.4 \times 10^{-8}$ M. The open symbols represent the data not used in the fit as they were not consistent with the model of a single apparent pK_a.

dependence of Figure 1 provides a reasonable representation of the intrinsic pH dependence (see Figure 5 below).

Effects of Specific Ions and Ionic Strength on the pH Dependence of $(k_{cat}/K_m)^{S,app}$ for Reaction of −1r,dS. Different buffers used in overlapping pH regions in Figure 1 gave similar rate constants, suggesting that specific buffer effects do not have a large effect on the observed pH dependence. However, each buffer at each pH contained different concentrations of unprotonated buffer, protonated buffer, and sodium counterion. The effects of these different concentrations and ionic strengths were investigated by first determining $(k_{cat}/K_m)^S$ for reaction of −1r,dS at buffer concentrations ranging from 25 to 200 mM (Figure 2A). Increasing the buffer concentration, which also increased the concentration of the Na^+ counterion, decreased $(k_{cat}/K_m)^S$. However, varying the buffer concentration while maintaining constant Na^+ concentration had no significant effect on $(k_{cat}/K_m)^S$, indicating that the buffers are not inhibitory {20−125 mM buffer (acetate, MES, HEPES, and CHES) with $[Na^+]$ = 200 mM maintained by addition of NaCl; data not shown}. This suggests that the decrease in $(k_{cat}/K_m)^S$ with increasing buffer concentrations was due to the increased concentration of Na^+.

To test this directly and to determine if this effect arose from ionic strength or specific ion effects, the effect of different added salts on $(k_{cat}/K_m)^S$ was determined (Figure 2B). Addition of 200 mM of monovalent salt (LiCl, NaCl, KCl, or RbCl; open symbols) inhibited the rate of reaction in all cases relative to the rate with 50 mM sodium buffer and 50 mM total Na^+ (closed symbols). Figure 2B also reveals specific ion effects, with a larger inhibition seen for the smaller, more densely charged metal ions: LiCl > NaCl > KCl > RbCl. This trend would support models of competition with specific metal binding sites or binding of ions to inhibitory sites rather than a more general inhibitory effect of charge screening. (The differences in the effects of the ions at the pH extremes is consistent with model III below, as described in the Discussion.)

Scheme 1

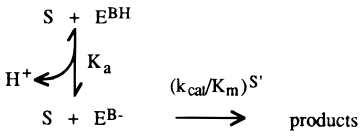

To avoid specific sodium ion effects, the pH dependence for $(k_{cat}/K_m)^S$ with the $[Na^+]$ held constant was used for analysis of the origin of the pH dependence (Figure 2C). Though conditions with 50 mM Na^+ and 10 mM Mg^{2+} were chosen, the pH dependence has the same shape at higher Na^+ (Figure 2B and data not shown). In addition, the shape was essentially unchanged in the presence of varying Mg^{2+} concentrations (3−50 mM, data not shown).

Analysis of pH Dependence of $(k_{cat}/K_m)^S$ for Reaction of −1r,dS. An initial step in the analysis of the pH dependence was to determine the value of the apparent pK_a. The simple model presented in Scheme 1, which illustrates that a proton must be lost for the reactants to be catalytically active, was assumed. Scheme 1 is represented mathematically by eq 1.

$$(k_{cat}/K_m)^S = (k_{cat}/K_m)^{S'}/\{([H^+]/K_a) + 1\} \qquad (1)$$

When eq 1 is fit to the data in Figure 2C, the value obtained for the apparent pK_a is 7.6.[2]

Models for the Origin of the Observed pH Dependence for Reaction of −1r,dS. Three models are addressed in dealing with the origin of the pH dependence for $(k_{cat}/K_m)^S$ for reaction of the −1r,dS substrate. These models are as

[2] Data at pH > 8.5 were omitted from the fit, as they cannot be accounted for by a single apparent pK_a. These data are discussed with model III below.

Scheme 2

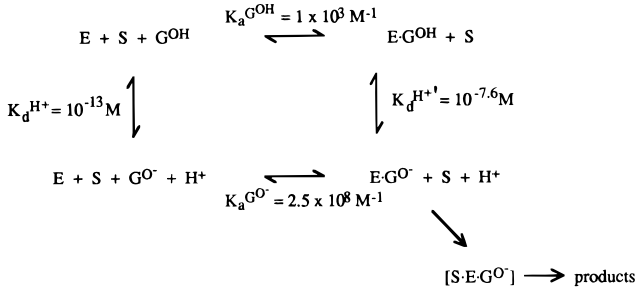

follows: (I) the ribozyme active site lowers the pK_a of the 3′-OH of the attacking G to 7.6; (II) the rate-limiting step changes from a pH-dependent to a pH-independent step, giving a kinetic pK_a of 7.6; and (III) there are multiple independent deprotonations with pK_a's higher than the apparent pK_a of 7.6, each of which inactivates the ribozyme. Evidence is presented against models I and II. A model in which titration of a group other than one on the attacking G is responsible for the observed pK_a of 7.6 cannot be ruled out; such a model cannot account for all of the data, however. Model III is the only one consistent with all of the data, and further evidence in support of this model is also described.

Test of Model I: Is the Apparent pK_a of 7.6 Due to Deprotonation of the of the Attacking G? A simple explanation for the apparent pK_a of 7.6 is that it represents the titration of a specific group on the ribozyme or substrate that must be deprotonated to allow reaction (Scheme 1). Although there are no groups on RNA with pK_a values around neutrality in solution (with the closest values being 4.5 and 9.4; Saenger, 1983), the values could be perturbed by the environment of the ribozyme. An obvious candidate is the 3′-OH of the attacking G, as this group must lose a proton in the course of the reaction and deprotonation could facilitate the reaction by increasing the nucleophilicity of the attacking G (Scheme 2). This model can be easily tested because it predicts that the binding of G gets stronger as the pH is increased [$(K_a^G)_{obsd}$, eq 2, derived from Scheme 2]. This occurs because in order to lower the pK_a of the 3′-hydroxyl of G, the ribozyme must bind more strongly to G^{O^-} than to G^{OH} (Scheme 2, eq 3).

$$K_a^G = (K_a^G)_{obsd} = K_a^{G^{OH}}\{1 + (K_d^{H+'}/[H^+])\} \quad (2)$$

$$K_d^{H+'}/K_d^{H^+} = K_a^{G^{O^-}}/K_a^{G^{OH}} \quad (3)$$

If the pK_a of 7.6 is *assumed* to represent the titration of the 3′-OH of G, then $K_a^{G^{O^-}}$ and the pH dependence of G binding can be predicted quantitatively as follows: (1) the values for $K_a^{G^{OH}}$ and $K_d^{H^+}$ are known from previous work (McConnell et al., 1993; Saenger, 1983), (2) the value of $10^{-7.6}$ M for $K_d^{H+'}$ was again assumed from the apparent pK_a of 7.6 (Figure 2C), and (3) these values and eq 3 were used to obtain the predicted value of $K_a^{G^{O^-}} = 2.5 \times 10^8$ M^{-1}, completing the thermodynamic box of Scheme 2.

Model I was therefore tested by measuring the observed value of K_a^G at different pH values (eq 2). Figure 3A shows representative binding curves for G at three different pH values, and Figure 3B displays the K_a^G values obtained from these binding curves as a function of pH. The observed binding did not get tighter as pH is increased; instead it

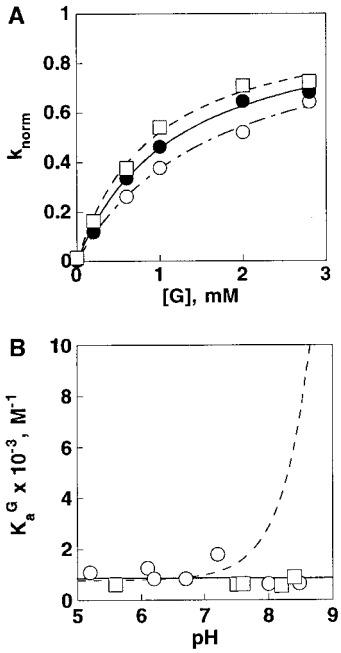

FIGURE 3: The absence of stronger binding of G with increasing pH indicates that the apparent pK_a of 7.6 for the pH dependence of −1r,dS is not due to the deprotonation of the 3′-OH of G. (A) G concentration dependence of −1r,dS cleavage at pH 5.2, □ (NaMES); 6.7, ● (NaMES); and 7.5, ○ (NaMOPS) (50 mM buffer, 0−2.6 mM G, 100−300 nM E, 10 mM $MgCl_2$, 50 °C). The lines represent nonlinear least-squares fits to a simple binding curve (Michaelis−Menten equation) and give $K_a^G = 1.1 \times 10^3$, 0.83×10^3, and 0.59×10^3 M^{-1} at pH 5.2, 6.7, and 7.5, respectively. The rate constants were normalized such that $k_{norm} = 1$ corresponded to the rate constant with saturating G obtained from the individual fits. (B) K_a^G as a function of pH. Values from A and analogous experiments. ○ represents a single determination as in A, and □ represents the average of two independent determinations. The average standard deviation for the K_a^G measurements obtained from two independent determinations was ±0.2 mM^{-1}. The solid line is drawn at 0.8×10^3 M^{-1}, which is the average value of K_a^G. It represents the predicted behavior if K_a^G is independent of pH over this range. The dashed line illustrates the predicted change in K_a^G according to model I (Scheme 2, eq 2), in which the deprotonation of the 3′-OH of G is responsible for the observed pK_a of 7.6.

remained constant at 0.8×10^3 M^{-1} up to pH 8.5 (Figure 3B). In contrast, model I predicts that the binding increases substantially (Figure 3B, dashed line). For example, the predicted value of $K_a^G = 7.9 \times 10^3$ M^{-1} at pH 8.5 is 10-fold greater than the observed average value of 0.8×10^3 M^{-1}, providing strong evidence against model I. While deprotonation of the 3′-OH of G does not appear to be responsible for the apparent pK_a of 7.6, it may nevertheless be responsible for the slope of one if its deprotonation is required for reaction. Its pK_a must be > 8, however. Something else must therefore cause the rate to level off above pH 7.6 as observed in Figure 2C.

Though it is not possible to test each of the ribozyme and substrate functional groups for a perturbed pK_a, a second obvious candidate is the 5′-triphosphate. This group is attached at the start of the IGS and therefore could lie in or near the active site. However, the same pH dependence and apparent pK_a were observed in reactions using a ribozyme with a 5′-OH replacing the 5′-triphosphate (data not shown), indicating that the 5′-triphosphate is not responsible for the observed pK_a.

Test of Model II: Is a Change in the Rate-Limiting Step Responsible for the Apparent pK_a? A second model which

could account for the apparent pK_a of 7.6 is a change in rate-limiting step from one that is pH dependent to one that is pH independent. This is depicted in Scheme 3 for a pH-dependent chemical step and a pH-independent conformational step. It should be noted that eq 4, representing model

Scheme 3

$$E{\cdot}G + S \overset{K_d^S}{\rightleftharpoons} (E{\cdot}G{\cdot}S) \xrightarrow{k_{conf}} (E{\cdot}G{\cdot}S)' \xrightarrow{k_{chem}/[H^+]} \text{products}$$

$$(k_{cat}/K_m)^{S,app} = \{(k_{chem}k_{conf})/(k_{chem} + k_{conf}[H^+])\}/K_d^S \quad (4)$$

$$\text{thio-effect} = \frac{\{(k_{chem}^O k_{conf})/(k_{chem}^O + k_{conf}[H^+])\}/K_d^S}{\{(k_{chem}^S k_{conf})/(k_{chem}^S + k_{conf}[H^+])\}/K_d^S} = \frac{(k_{cat}/K_m)^{S,Oxygen}}{(k_{cat}/K_m)^{S,Sulfur}} \quad (5)$$

II, has the same mathematical form as eq 1, representing model I, so that the fits are equivalent and cannot be used to differentiate between these models.

One way to test for a change in rate-limiting step for the *Tetrahymena* ribozyme is to use a phosphorothioate substrate, in which a sulfur atom replaces a nonbridging phosphoryl oxygen atom at the cleavage site. This approach has been used previously to identify a pH-independent conformational change for reaction of this ribozyme with the all-ribose substrate (rS, Chart 1): in that case, thio substitution slowed the rate of the chemical step ~2−3-fold for the all-ribose substrate (rS), while having no significant effect on binding or conformational steps (Herschlag et al., 1991; Herschlag & Khosla, 1994).

Thio substitution was therefore employed to probe the rate-limiting step for the −1r,dS reaction as a function of pH (Figure 4A). The thio-effect is constant and greater than 1, consistent with a rate-limiting chemical step over the entire pH range 6.2−8.4. In contrast, if a change in rate-limiting step, analogous to that depicted in Scheme 3, were responsible for the apparent pK_a of 7.6, the thio-effect would be predicted to drop to 1.0 at high pH (Figure 4A, dashed line). These results therefore provide evidence against a change in rate-limiting step that is responsible for the observed pK_a.

The thio-effect for the −1r,dS reaction is small, only 1.8, and the maximal value of $(k_{cat}/K_m)^S$ for the −1r,dS substrate of ~10^7 M^{-1} min^{-1} approaches values of ~10^8 M^{-1} min^{-1} previously determined for binding of oligonucleotide substrates to the ribozyme (Herschlag & Cech, 1990; Herschlag et al., 1993b). Though a change to a rate-limiting binding step would also be predicted to give a change to a thio-effect of 1 (Herschlag, 1992; Herschlag & Khosla, 1994), we wanted to provide an independent test of this and the conformational change model of Scheme 3. These possibilities were therefore tested with another substrate, dS. The pH dependence for $(k_{cat}/K_m)^S$ for dS followed the same shape as that for −1r,dS (not shown). As this substrate reacts much slower than −1r,dS (~10^3-fold; Herschlag et al., 1993b), the possibility of a change to a rate-limiting binding step at high pH is eliminated. Further, the thio-effect is slightly larger with a deoxyribose residue than a ribose residue at the cleavage site, allowing a more sensitive probe for a change in rate-limiting step. A thio-effect of 2.3 was observed for

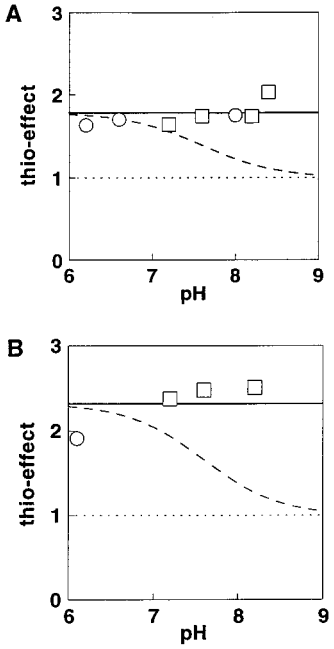

FIGURE 4: The absence of a change in thio-effect with increasing pH suggests that the rate plateau in $(k_{cat}/K_m)^S$ at high pH is not due to a change in rate-limiting step for −1d,rS (A) and dS (B). (A) Thio-effect for reaction of −1r,dS as a function of pH (50 mM sodium buffer, 50−100 nM E, 2 mM G, 10 mM $MgCl_2$, 50 °C): determination in triplicate, ○; average of two independent triplicate determinations, □. The average standard deviation for measurements obtained from two independent determinations is ±0.3. The solid line represents a thio-effect of 1.8, which is the average of the observed thio-effects. The dashed line represents the effect of pH on the thio-effects predicted by model II (Scheme 3) as was obtained from eq 5 and the following: (1) k_{conf} and K_d^S were assumed to be the same for the oxygen and sulfur substrates (Herschlag & Khosla, 1994; Herschlag et al., 1991); (2) values of k_{chem}^O/K_d^S = 0.084 min^{-1} and $k_{conf}/K_d^S = 3.5 \times 10^6$ M^{-1} min^{-1} were obtained from a nonlinear least-squares fit of the observed pH dependence of Figure 2C to eq 4; and (3) k_{chem}^S/K_d^S = 0.047 min^{-1} was obtained from k_{chem}^O/K_d^S = 0.084 min^{-1} and the observed average thio-effect of 1.8. (B) Thio-effect for reaction of dS as a function of pH (50 mM sodium buffer, 300−400 nM E, 2 mM G, 10 mM $MgCl_2$, 50 °C): determination in multiplicate, ○; average of two independent multiplicate determinations, □. The average standard deviation for measurements obtained from two separate determinations is ±0.5. The solid line represents a thio-effect value of 2.3, the average of the observed thio-effects. The dashed line represents the effect of pH on the thio-effects predicted by model II (Scheme 3) and was obtained as described in A.

dS throughout the pH range (Figure 4B), providing further evidence against a change to a rate-limiting conformational step at high pH.

Neither Model I nor II is Consistent with the Decrease in $(k_{cat}/K_m)^{S,app}$ at High pH. Evidence against both models I and II was presented above. In addition, neither of these models nor a model invoking titration of a single ribozyme functional group can explain the decrease in $(k_{cat}/K_m)^{S,app}$ at high pH (Figure 2C). One simple explanation could be that this decrease is due to ribozyme degradation, but precautions were taken to minimize degradation using the pH jump method and controls suggested that degradation was not a problem (see Materials and Methods).

Model III: Multiple Independent Deprotonations Are Capable of Inactivating the Ribozyme. A third model that can account for all regions of the pH dependence (slope of 1, leveling off, and the drop at high pH) is that there are multiple independent deprotonations, each of which inacti-

Scheme 4

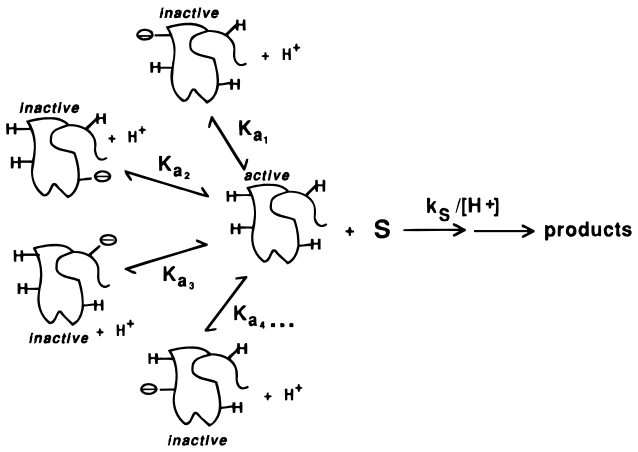

vates the ribozyme, and that the pK_a's are far removed from the apparent pK_a of 7.6 (Scheme 4). The pH dependence predicted for a simplified version of Scheme 4 is represented by eq 6, in which all n groups that inactivate the ribozyme

$$(k_{cat}/K_m)^{S,app} = \{k_S/[H^+]\}\{(1/(1 + (K_a/[H^+])))^n\} \quad (6)$$

upon proton loss are assumed to have the same pK_a [i.e., K_a (in eq 6) $= K_{a_1} = K_{a_2} =$ ... from Scheme 4; k_S is defined in Scheme 4 as the pH-independent rate constant for reaction of E·(G) + S]. Equation 6 was derived with the simplifying assumption that each deprotonation has no effect on the other deprotonations, i.e., that the independence is absolute. The nth-order dependence in eq 6 arises not from cooperative deprotonation or protonation but rather from the requirement that all n sites be protonated in order for the reaction to occur.

The solid line in Figure 5 shows that this model provides a good fit to the observed pH dependence, giving an estimate of 19 groups with pK_a 9.4. The pK_a value of 9.4 was assumed in this fit because it represents the lowest pK_a of RNA in the basic region; 9.4 is the pK_a of N3 of U and N1 of G free in solution (Saenger, 1983). These groups are more likely to be deprotonated than groups with higher pK_a values and therefore are expected to play a larger role in the observed inactivation.

Though the fit of the pH dependence to eq 6 suggests that model III can account for the observed pH dependence, the value $n = 19$ obtained for the number of protons whose loss inactivates the ribozyme is only a crude estimate for the following reasons: (1) The actual pK_a's of essential groups can vary due to the environment surrounding each titrating group. (2) Groups with pK_a's higher than 9.4 will also contribute to the loss of activity at high pH, with the extent of their contribution decreasing with increasing pK_a. (3) The loss of certain protons may only partially inactivate the ribozyme. Assuming a pK_a value of 9.1 or 9.7 instead of 9.4 gave good fits to the data with $n = 10$ and 36, respectively (not shown). This underscores the difficulty in determining precise numbers of titratable groups and their individual pK_a values. Nevertheless, inactivation from ≈20 titratable groups appears reasonable (see Discussion).

Effect of pH on the Stability of a Model P1 Duplex Provides Support for Model III. The loss of certain protons could decrease binding of S to the ribozyme. As S binding includes duplex formation, stabilities for a model duplex between −1r,dS and the oligonucleotide IGS′, which has the sequence of the ribozyme's IGS, were determined over a range of pH (Figure 6). There are five G's in the ribozyme's IGS (and in IGS′) and two U's in S (Figure 7A). N1 of G and N3 of U, which titrate with the pK_a of 9.4, are normally involved in base pairing. Thus, deprotonation of any of these seven candidates is predicted to prevent duplex formation. The stability of the model duplex is weakened at higher pH (Figure 6). The data fit a model in which deprotonation of four groups of pK_a 9.4 prevents duplex formation (eq 7, derived analogously to eq 6). This is in reasonable agreement with the predicted involvement of seven protons, given

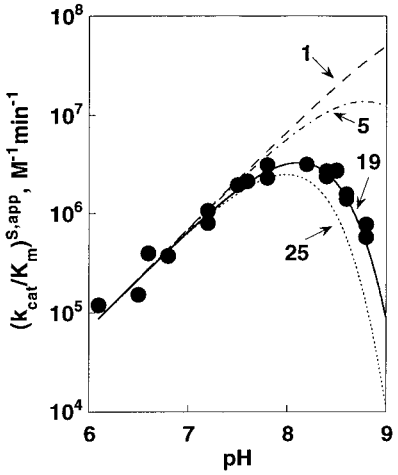

FIGURE 5: The pH dependence for cleavage of −1r,dS at constant Na^+ concentration (2 mM G, 100 nM E, 10 mM $MgCl_2$, 50 °C). The reactions were carried out at 50 mM sodium buffer, with NaCl added to a total of 50 mM Na^+. (The pH jump method was used to avoid problems from ribozyme degradation at high pH; see Materials and Methods.) The solid line represents the nonlinear least-squares fit to the data for model III, in which the loss of protons from side chains of pK_a ~9.4 inactivate the ribozyme to give $k_S = 0.070$ min^{-1} and $n = 19$ for the number of titratable groups that lead to inactivation (eq 6; k_S is the pH-independent, second-order rate constant for reaction of the active form of the ribozyme with S, as depicted in Scheme 4). The dotted and dashed lines shown for comparison represent curve fits in which $k_S = 0.070$ min^{-1} and the number of protons which lead to inactivation was fixed at $n = 1$, 5, or 25.

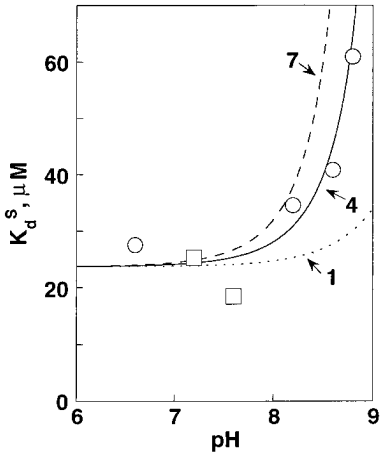

FIGURE 6: The effect of pH on the dissociation constant for the −1r,dS·GGAGGGA (IGS′) duplex. The substrate inhibition method was employed, as described in the Materials and Methods (50 mM sodium buffer, 10 mM $MgCl_2$, 50 °C). The solid line represents a least-squares fit to eq 7, giving a value of four protons and with assumed pK_a values of 9.4 on the IGS′ or substrate strands that disrupt duplex formation ($K_d^S{}_{intrinsic} = 24$ μM). For comparison, the dashed lines show the dependence expected if seven or one protons with pK_a 9.4 are lost.

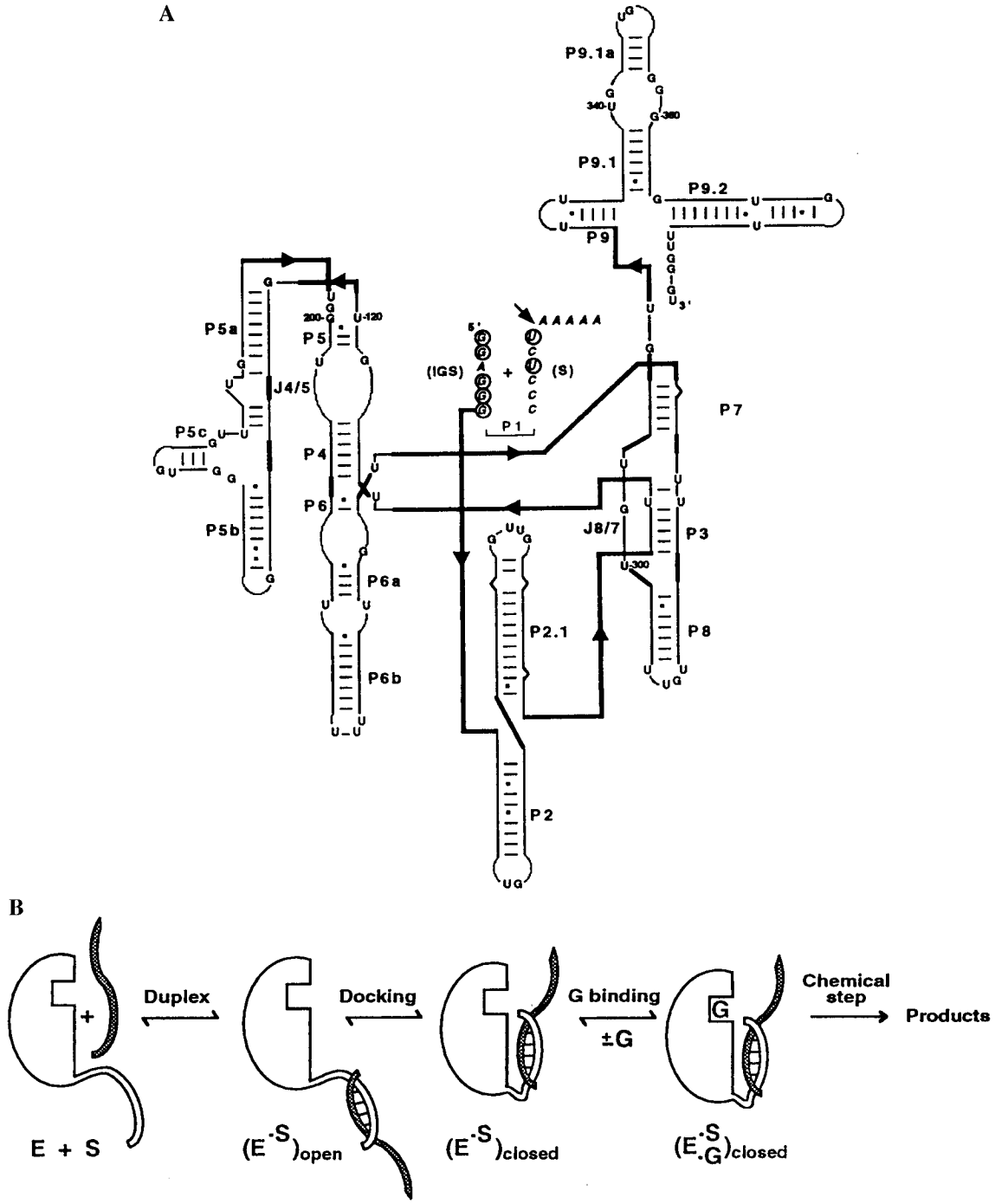

FIGURE 7: *Tetrahymena* ribozyme and its reaction. (A) Position of G's and U's in the secondary structure of the *Tetrahymena* ribozyme (Michel & Westhof, 1990). Only the G's and U's in nonduplex regions of the secondary structure are shown explicitly, except for the ribozyme's internal guide sequence (IGS) and the oligonucleotide substrate (S), which are shown in italics with their G's and U's circled [modified from Cech et al. (1994)]. The IGS and S pair to form the P1 duplex. (B) Individual steps in the *Tetrahymena* ribozyme reaction. The first step is formation of the P1 duplex between S and the IGS of the ribozyme; this duplex then docks into tertiary interactions with the ribozyme's core. Evidence for the individual steps has been reviewed previously (Cech et al., 1992; Cech & Herschlag, 1996). Modified from Knitt et al. (1994).

$$K_d^S = K_{d\ intrinsic}^S(1 + (K_a/[H^+]))^n \quad (7)$$

the small size of the effect over the observed pH range and the simplifying assumptions stated above.

The experiments described above that disprove models I and II are consistent with model III. The fact that the thio-effect is constant over the observed pH range suggests that the same step of the reaction remains rate limiting at all pH's, consistent with model III. At pH values greater than 8.5 the binding of G weakened (data not shown). This is consistent with model III, as deprotonation of N3 of the nucleophilic guanosine and deprotonation of G's and U's in the ribozyme's guanosine binding site could prevent guanosine binding. Six groups titrating with pK_a 9.4 would give a 2-fold decrease in binding at pH 8.5, though it was not possible to ascertain the precise extent of weakened binding due to limits of guanosine solubility.

pH Dependence of $(k_{cat}/K_m)^G$ *for Reaction of* $-1d,rS$ *Provides Further Support for Model III.* According to model III, binding and docking of S would elevate the pK_a's of the

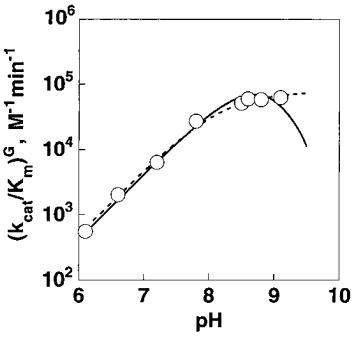

FIGURE 8: pH dependence for cleavage of −1d,rS [$(k_{cat}/K_m)^G$, 50 mM sodium buffer, 0−20 μM G, 200 nM E, 10 mM $MgCl_2$, 50 °C]. The solid line and dashed line represent nonlinear least-squares fits to the data for model III (eq 6) and an apparent pK_a (eq 1), respectively, except that the reactions were followed under subsaturating G and saturating substrate conditions, $(k_{cat}/K_m)^G$ instead of $(k_{cat}/K_m)^{S,app}$, with the term k_G used instead of k_S (k_G is then the pH-independent rate constant for reaction of the active form of the E·S complex and G, as depicted in Scheme 4 with G replacing S). Model III (eq 6) gave values of $k_G = 0.0004$ min^{-1} and $n = 6$ for the number of titratable groups which lead to inactivation. The fit to a single pK_a (eq 1) gave values of $(k_{cat}/K_m)^{G'} = 7.7 \times 10^4$ M^{-1} min^{-1} and p$K_a = 8.2$.

G's and U's on the IGS and S, as well as the pK_a's of ribozyme groups required for docking (Figure 7B). These groups would then no longer have a significant effect on reactivity in the observed pH range. Thus, a reaction that begins with S already bound and docked is predicted to exhibit less of a rate decrease at high pH. Figure 8 shows the pH dependence for E·S + G → products, $(k_{cat}/K_m)^G$, for reaction of −1d,rS. These data are best fitted with six groups of pK_a 9.4 whose deprotonation inactivates the E·S complex. Thus, fewer protons affect reaction of the E·S complex than reaction of free E. The difference in the behavior of free E and S and the E·S complex is also demonstrated by the higher apparent pK_a of 8.2 for the E·S reaction compared to the apparent pK_a of 7.6 for reaction of E and S (Figure 5 and 8, fit to eq 1).[3]

DISCUSSION

A kinetic and thermodynamic framework was previously established for individual steps of the reaction of the *Tetrahymena* ribozyme at a single pH (Herschlag & Cech, 1990). In subsequent studies, an apparent pK_a of 7 was observed for reaction of the cognate, all-ribose substrate. Because RNA contains no groups that titrate near neutrality, the possibility that the ribozyme perturbed the pK_a of a catalytic functional group was introduced. However, this apparent pK_a was shown to arise from a change in rate-limiting step rather than from an actual titration (Herschlag & Khosla, 1994). The somewhat higher apparent pK_a observed for reaction of a slower substrate, −1r,dS, suggested that a catalytic group with a pK_a perturbed to near neutrality might nevertheless be present (Herschlag et al., 1993b). The pH study reported herein was undertaken to understand the origin of this apparent pK_a and, more generally, to understand how pH can affect the behavior of RNA catalysts and what experimental precautions are required to obtain a valid pH profile. The results suggest that this apparent pK_a does not arise either from titration of a catalytic group or from a change in rate-limiting step but rather arises from independent titrations of the RNA bases, which have pK_a's greater than the observed apparent pK_a.

Effects of Specific Ions and Buffers on the pH Dependence. To ensure that the observed pH dependence accurately reflected the intrinsic effect of protonation on the ribozyme reaction, controls for effects of specific ions, buffer components, and ionic strength were carried out. In this case, no specific buffer effects were observed, but there was inhibition by specific cations ($Li^+ > Na^+ > K^+ > Rb^+$). Presumably the smaller ions are more effective inhibitors because of stronger interactions with the charged phosphodiester backbone. The pH dependence was therefore carried out in the presence of a constant concentration of a single cation. More generally, carrying out pH-dependence experiments for RNA reactions with constant cation concentration and including different buffers with overlapping pH values will help prevent the appearance of artifacts from specific salt effects and will help identify effects from specific buffers. Using high concentrations of salt may also minimize effects from changes in salt and buffer as pH is varied. Salt or buffer effects may have skewed previously observed pH dependencies of RNA catalysts that did not fit a simple theoretical dependence with an integer slope (Dahm et al., 1993; Weeks & Cech, 1995).

An Unconventional Origin for an Apparent pK_a. Two explanations are typically presented to account for apparent pK_a's: titration of a functional group or a change in rate-limiting step from one that is pH dependent to one that is pH independent. The pH dependence for the reactions investigated herein did not appear to fit either of these categories. However, another mechanism that is expected to be common for RNA at higher pH values is the loss of protons due to the titrations of RNA functional groups (Dahm et al., 1993). A leveling off and subsequent drop at high pH values could result from several independent deprotonations with each individual proton loss leading to inactivation of the ribozyme; these individual effects combine to give an apparent pK_a that is far removed from the actual pK_a values of the functional groups, followed by a decrease in rate at higher pH values (Scheme 4 & model III from Results).

The pH dependence for reaction of the oligonucleotide substrate −1r,dS was fitted to a simplified version of this unconventional model in which each of the titrating groups had pK_a's of 9.4, the unperturbed pK_a of N1 of G and N3 of U, and gave a dependence on 19 titratable groups (Figure 5). There are enough G's and U's in nonduplex regions of the *Tetrahymena* ribozyme (~60, Figure 7A) to account for this dependence. Some of these G's and U's may have their pK_a's perturbed to higher values from tertiary interactions and would therefore play a smaller role in the observed pH

[3] The apparent pK_a of 7.6 was determined for the reaction of E·G with S. The observation that the binding of G is not affected from pH 5.2−8.5 indicates that reactions involving free E (i.e., E + G + S → $[E·G·S]^‡$) follow the same apparent pK_a. Different chimeric substrates were used to follow the E + S and the E·S reactions; these are used because their different binding affinities and reactivities allow different reaction steps to be followed conveniently. The effects of individual 2′ hydroxyl groups on binding and reactivity are well-understood (Bevilacqua & Turner, 1991; Pyle & Cech, 1991; Herschlag et al., 1993a,b; McConnell et al., 1993; G. J. Narlikar and D. Herschlag, unpublished results) and are not expected to affect the conclusions.

dependence.[4] Also, the ribozyme would not be expected to require a proton on all of these G's and U's for activity, especially those removed from the catalytic core.

Additional experiments provided support for this mechanism of inactivation. These experiments, combined with previous structural and functional data, suggested the identity of some of the protons required in individual reaction steps (Figure 7B). The first step is formation of the P1 duplex between the oligonucleotide substrate and the ribozyme's IGS to give the open complex [$(E^{\cdot S})_{open}$]. As the substrate and IGS contain a total of five G's and two U's (Figure 7A), a dependence on seven titratable groups of pK_a 9.4 was expected. The formation of a model P1 duplex gave a best fit to a dependence on four groups, which is in reasonable agreement with the expected value of 7 given the small size of the effect and the assumptions involved (Figure 6 and Results).

It was predicted that the pH dependence of a reaction starting with the P1 duplex already formed and docked into its tertiary interactions [$(E^{\cdot S})_{closed}$, Figure 7B] would involve fewer titratable groups. This is expected because the titratable groups involved in duplex formation and docking would have pK_a's perturbed to higher values and therefore have a smaller effect in the observed pH range. The observed dependence on six protons rather than 19 confirmed this prediction [Figure 8, reaction of E·(−1d,rS); $(k_{cat}/K_m)^G$]. One of these six protons is presumably N1 of the G nucleophile, which donates a hydrogen bond to O6(G) of the conserved G264·C311 base pair in the G binding site (Michel et al., 1989). Guanosine binding is indeed weakened above pH 8.5, though the extent of this effect could not be determined due to the low solubility of G. The remaining five titratable groups estimated to affect $(k_{cat}/K_m)^G$ for the −1d,rS substrate could be ribozyme groups involved in G binding or in the chemical step.

Of the 19 titratable groups estimated to affect the overall reaction, four to seven groups have been implicated in duplex formation and approximately six groups subsequent to docking. This leaves an estimated six to nine titratable groups that are involved in docking of the P1 duplex into tertiary interactions (Figure 7B). Previous structural and functional studies have suggested that J8/7 and J4/5 are in the vicinity of the docked P1 duplex and may provide docking contacts (Michel & Westhof, 1990; Pyle et al., 1992; Wang et al., 1993). Thus the three G's and U's of J8/7 and two of J4/5 are candidates for this effect (Figure 7A). Finally, a trans splicing reaction of the *Tetrahymena* intron is slowed at lower pH values when the pK_a of the N3 position of U is lowered via replacement of the intron U's with 5-fluoro-U (Danenberg et al., 1989), consistent with model III.

The inactivating titrations could either remove a proton involved in a direct contact or indirectly affect the structure. The inability of increased Mg^{2+} to significantly perturb the apparent pK_a suggests that global unfolding is not responsible, however. In contrast, Mg^{2+} has been shown to rescue deleterious effects from many intron mutations (Flor et al., 1989; Beaudry & Joyce, 1990; Joyce et al., 1989; Jaeger et al., 1991; Mohr et at., 1994).

[4] Some G's and U's or other groups may instead have their pK_a's perturbed to lower values and therefore play a larger role in the observed pH dependence.

Ribozyme Inactivation Analogous to That Observed at High pH Is Predicted to Occur at Low pH. The mechanism of multiple independent deprotonations that influence the ribozyme's activity was discussed above for groups that titrate in the basic region. RNA also contains groups that titrate in the acidic region; N1 of A and N3 of C titrate at pH ∼4 (Saenger, 1983). Thus, an analogous mechanism of multiple independent inactivating protonations (rather than deprotonations) would be expected to inhibit the ribozyme's activity at low pH values. Evidence supporting this model at low pH includes the pH dependence breaking from a slope of one to a steeper slope below pH 6 [$(k_{cat}/K_m)^S$ for −1r,dS] and the affinity of G for the E·S complex decreasing below pH 6 (D. S. Knitt and D. Herschlag, unpublished results). In addition, perturbation of the pK_a's of the inactivating groups may be responsible for the differences in specific salt effects at both the low and high pH extremes (Figure 2A,B).

Multiple Independent Deprotonations As a General Mechanism for Inactivation of Functional RNAs. The mechanism of multiple independent deprotonations (or protonations) leading to inactivation is expected to hold for functional RNAs in general. Each RNA base contains a group that titrates at pH ∼9 or ∼4, in contrast to proteins, which have only a fraction of side chains with pK_a's in the region 4−9. Additionally, RNA contains no groups with unperturbed neutral pK_a's whereas pH dependencies for proteins are often dominated by side chains that titrate near neutrality.

Indeed, pH−rate profiles for the hammerhead ribozyme (Dahm et al., 1993), RNase P RNA (Smith & Pace, 1993), and a group II derived ribozyme (Pyle & Green, 1994) level off in the pH 7−9 region. The pH dependencies for these functional RNAs do not all level off at the same pH value, which is expected as the RNAs differ in size and active site environments. The higher apparent pK_a observed for the small hammerhead ribozyme versus the larger and more complex *Tetrahymena*, RNase P, and group II ribozymes is consistent with these general expectations.

For the RNase P ribozyme, apparent pK_a's of ∼8 in pH−rate profiles were suggested to arise from titration to form a nucleophilic $Mg{\cdot}OH^+$ species, with the pK_a lowered from its normal value of 11.4 by the active site environment (Smith & Pace, 1993; Baes & Mesmer, 1976). A prediction of this proposal applied to the group I reaction is that the binding of the nucleophilic G increases as pH increases. This prediction was tested and disproved for the *Tetrahymena* ribozyme (Figure 3). The analogous experiment cannot be carried out with RNase P because the concentration of the water nucleophile cannot be varied in a controlled manner. However, the similar apparent pK_a for the RNase P reaction in Mg^{2+} and in Ca^{2+} is not simply reconciled with participation of a nucleophilic $Mg{\cdot}OH^+$ or $Ca{\cdot}OH^+$, as these species have different intrinsic pK_a's. Inactivation of RNase P from multiple independent deprotonations, as described herein for the *Tetrahymena* ribozyme, could account for these apparent pK_a's.

pH Dependencies Provide Mechanistic Insights into the Tetrahymena Ribozyme Cleavage Reaction. The pH−rate profiles determined in this study confirm and extend conclusions from preliminary pH−rate profiles that were obtained prior to performing the rigorous controls described herein (Herschlag et al., 1993b; Herschlag & Khosla, 1994).

(i) The slope of one observed in the pH−rate profiles below pH ∼8 indicates that a proton is lost before the rate-

limiting step. There is strong evidence that this rate-limiting step is the chemical step [summarized in Herschlag et al. (1993b)].

(ii) The results of Figure 3 showed that the pK_a of the 3′-OH of G is not lowered below 8. However, the 3′-OH could still be perturbed. An interaction with Mg^{2+} or another ribozyme group could lower its pK_a to a lesser extent. The Mg ion that interacts with the 3′-OH of the oligonucleotide product presumably lowers its pK_a (Piccirilli et al., 1993; Narlikar et al., 1995), but binding data analogous to that presented here for G suggest that this pK_a remains ≥ 9 (unpublished results).

(iii) More generally the results indicate that the pK_a of any group that must be deprotonated prior to the chemical step is greater than 8.2, the apparent pK_a observed in Figure 8. The actual pK_a of the 3′-OH of the bound G nucleophile or of a general base that deprotonates the 3′-OH is likely to be significantly greater than 8, because deprotonations of several groups with higher pK_a's presumably contribute to this apparent pK_a. Though we and others still favor a mechanism that involves metal ion activation of the 3′-OH of the G nucleophile (Yarus, 1993; Steitz & Steitz, 1993; Herschlag et al., 1993a; Herschlag & Khosla, 1994), there are as yet no data that distinguish between metal ion and general base catalysis.

ACKNOWLEDGMENT

We thank Mala Khosla for technical and other assistance throughout this project, Scott Strobel for a generous gift of ribozyme lacking the 5′-triphosphate, Sylvester Muthini (Clontech) for oligonucleotide synthesis, Geeta Narlikar and Alessio Peracchi for many helpful discussions, and members of the Herschlag laboratory for helpful comments on the manuscript.

REFERENCES

Baes, C. F. J., & Mesmer, R. E. (1976) *The Hydrolysis of Cations*, Wiley, New York.
Beaudry, A., & Joyce, G. F. (1990) *Biochemistry 29*, 6534−6539.
Bevilacqua, P. C., & Turner, D. H. (1991) *Biochemistry 30*, 10632−10640.
Cech, T. R., & Herschlag, D. (1996) *Nucleic Acids and Molecular Biology: Special Issue on RNA Catalysis*, Springer-Verlag, New York (in press).
Cech, T. R., Damberger, S. H., & Gutell, R. R. (1994) *Struct. Biol. 1*, 273−280.
Dahm, S. C., Derrick, W. B., & Uhlenbeck, O. C. (1993) *Biochemistry 32*, 13040−13045.
Danenberg, P. V., Shea, L. C. C., & Danenberg, K. (1989) *Biochemistry 28*, 6779−6785.
Flor, P. J., Flanegan, J. B., & Cech, T. R. (1989) *EMBO J. 8*, 3391−3399.
Good, N. E., Winget, D., Winter, W., Connolly, T. N., Izawa, W., & Singh, R. M. M. (1966) *Biochemistry 5*, 467−477.
Gueffroy, D. E., Ed. (1978) *Buffers. A guide for the preparation and use of buffers in biological systems*, Calbiochem-Behring Corp, LaJolla, CA.
Herschlag, D. (1992) *Biochemistry 31*, 1386−1399.
Herschlag, D., & Cech, T. R. (1990) *Biochemistry 29*, 10159−10171.
Herschlag, D., & Khosla, M. (1994) *Biochemistry 33*, 5291−5297.
Herschlag, D., Piccirilli, J. A., & Cech, T. R. (1991) *Biochemistry 30*, 4844−4854.
Herschlag, D., Eckstein, F., & Cech, T. R. (1993a) *Biochemistry 32*, 8299−8311.
Herschlag, D., Eckstein, F., & Cech, T. R. (1993b) *Biochemistry 32*, 8312−8321.
Jaeger, L., Westhof, E., & Michel, F. (1991) *J. Mol. Biol. 221*, 1153−1164.
Joyce, G. F., van der Horst, G., & Inoue, T. (1989) *Nucleic Acids Res. 17*, 7879−7889.
Knitt, D. S., Narlikar, G. J., & Herschlag, D. H. (1994) *Biochemistry 33*, 13864−13879.
Kruger, K., Grabowski, P. J., Zaug, A. J., Sands, J., Gottschling, D. E., & Cech, T. R. (1982) *Cell 31*, 147−157.
Latham, J. A., & Cech, T. R. (1989) *Science 245*, 276−282.
McConnell, T. S., Cech, T. R., & Herschlag, D. (1993) *Proc. Natl. Acad. Sci. U.S.A. 90*, 8362−8366.
Michel, F., & Westhof, E. (1990) *J. Mol. Biol. 216*, 585−610.
Michel, F., Hanna, M., Green, R., Bartel, D. P., & Szostak, J. W. (1989) *Nature 342*, 391−395.
Mohr, G., Caprara, M. G., Guo, Q., & Lambowitz, A. M. (1994) *Nature 370*, 147−150.
Narlikar, G. J., Gopalakrishnan, V., McConnell, T. S., Usman, N., & Herschlag, D. (1995) *Proc. Natl. Acad. Sci. U.S.A. 92*, 3668−3672.
Piccirilli, J. A., Vyle, J. S., Caruthers, M. H., & Cech, T. R. (1993) *Nature 361*, 85−88.
Pyle, A. M., & Cech, T. R. (1991) *Nature 350*, 628−631.
Pyle, A. M., & Green, J. B. (1994) *Biochemistry 33*, 2716−2725.
Pyle, A. M., Murphy, F. L., &Cech, T. R. (1992) *Nature 358*, 123−128.
Rajagopal, J., Doudna, J. A., & Szostak, J. W. (1989) *Science 244*, 692−694.
Saenger, W. (1983) *Principles of Nucleic Acid Structure*, Springer-Verlag, New York.
Smith, D., & Pace, N. R. (1993) *Biochemistry 32*, 5273−5281.
Steitz, T. A., & Steitz, J. A. (1993) *Proc. Natl. Acad. Sci. U.S.A. 90*, 6498−6502.
Wang, J., Downs, W. D., & Cech, T. R. (1993) *Science 260*, 504−508.
Weeks, K. M., & Cech, T. R. (1995) *Biochemistry 34*, 7728−7738.
Yarus, M. (1993) *FASEB J. 7*, 31−39.
Zaug, A. J., Grosshans, C. A., & Cech, T. R. (1988) *Biochemistry 27*, 8924−8931.

BI9521147